that the bands between 850 and 1100 cm^{-1} may be tentatively assigned to stretching vibrations of this portion of the molecules.

Ultraviolet Spectra. Ultraviolet spectral data for the (pentane-2,4-dionato)phosphorus(V) compounds are presented in Table IX. All of the complexes show a strong single absorption between 270 and 310 nm, which appears to relate to the characteristic strong band of the $\pi-\pi^*$ electronic transition[27,28] of the free pentane-2,4-dione at 275 nm. There are no direct parallels with metal complexes because most such systems have several pentane-2,4-dionato chelates with a resultant splitting of the π levels of the ligand. The range of transition energies demonstrated by the series can be attributed to the electrostatic effects of the other ligands on the phosphorus, which suggests some involvement of phosphorus d orbitals with the π structure of the chelate. The π HOMO and π^* LUMO can only experience such effects via interaction with the empty d_{xz} and d_{yz} orbitals of the phosphorus. There is no obvious trend to the observed energies throughout the series, but it is notable that there seems to be a regular trend of increasing λ_{max} from $F_4P(acac)$ to $F_2(CF_3)_2P(acac)$ (i.e., with increasing CF_3 substitution) that is broken by $F(CF_3)_3P(acac)$. As shown by the crystal structure, this molecule exhibits a rather unusual bending of the acac ligand, which may account for the anomaly. The fact that anomalous behavior is exhibited by the visible spectrum in solution may indicate that the bending of the substituent persists in solution and is a molecular effect rather than a crystal-packing effect.

Mass Spectra. The major mass spectral peaks observed for the (pentane-2,4-dionato)phosphorus(V) compounds (except the isomeric mixture of II) are given in the Experimental Section. $F_4POC(CH_3)C(H)C(CH_3)O$ is the only member of the series that exhibits a parent ion, and it is further unique in showing the F_4P^+ ion as the most intense in the spectrum. In common with the case for five-coordinate phosphoranes[29] and the hexacoordinate carbamates,[2] the trifluoromethyl derivatives do not show a parent ion. In these cases the most intense peak is m/e 43, which corresponds to CH_3CO, a fragment of the chelate. As in the carbamato derivatives, the P–O bond is quite robust and many of the fragments can be identified as due to loss of only one CF_3 or F ligand from the parent molecule. In all cases a phosphonium ion is observed resulting from loss of the chelate.

Acknowledgment. We thank the Natural Sciences and Engineering Research Council of Canada for financial support.

Supplementary Material Available: Listings of anisotropic thermal parameters and least-squares planes (6 pages); tables of calculated and observed structure factors (23 pages). Ordering information is given on any current masthead page.

(28) Fackler, J. P.; Cotton, F. A.; Barnum, D. W. *Inorg. Chem.* **1963**, *2*, 97.

(29) Schmutzler, R. In *Halogen Chemistry*; Gutmann, V., Ed.; Academic: New York, 1967; Vol. 2, p 31.

Contribution from the Department of Chemistry, Memorial University of Newfoundland, St. John's, Newfoundland, Canada A1B 3X7, Chemistry Division, National Research Council, Ottawa, Ontario, Canada K1A 0R6, and Department of Chemistry, Drexel University, Philadelphia, Pennsylvania 19104

Structure and Electrochemical Properties of Antiferromagnetically Coupled Binuclear Hydroxo-Bridged Copper(II) Complexes with Pyridazine and Phthalazine Ligands. Crystal and Molecular Structures of [μ-3,6-Bis(1-pyrazolyl)pyridazine-N^2,μ-N^3,μ-N^4,N^5](μ-hydroxo)trichloroaquodicopper(II)-0.8-Water, $Cu_2C_{10}H_{11}Cl_3N_6O_2 \cdot 0.8H_2O$, [$\mu$-3,6-Bis(1-pyrazolyl)pyridazine-N^2,μ-N^3,μ-N^4,N^5](μ-hydroxo)tribromoaquodicopper(II)-0.6-Water, $Cu_2C_{10}H_{11}Br_3N_6O_2 \cdot 0.6H_2O$, and [$\mu$-1,4-Bis(1-methyl-2-imidazolyl)phthalazine](μ-hydroxo)tribromoaquodicopper(II)-Water, $Cu_2C_{16}H_{17}Br_3N_6O_3 \cdot H_2O$

Laurence K. Thompson,*[1a] Sanat K. Mandal,[1a] Eric J. Gabe,†[1b] Florence L. Lee,[1b] and Anthony W. Addison[1c]

Received June 17, 1986

The ligands 3,6-bis(1-pyrazolyl)pyridazine (PPD) and 1,4-bis(1-methyl-2-imidazolyl)phthalazine (MIP) form binuclear copper(II) complexes in which the square-pyramidal metal centers are bridged by a hydroxide and a diazine group (N-N). Large Cu–Cu separations (3.41–3.46 Å) and Cu–O(H)–Cu bridge angles (116–125°) are observed, and the complexes exhibit very low room-temperature magnetic moments indicative of strong spin exchange. The crystal and molecular structures of $[Cu_2(PPD)(OH)Cl_3(H_2O)] \cdot 0.8H_2O$ (I), $[Cu_2(PPD)(OH)Br_3(H_2O)] \cdot 0.6H_2O$ (II), and $[Cu_2(MIP)(OH)Br_3(H_2O)] \cdot H_2O$ (III) are reported. I crystallized in the triclinic system, space group $P\bar{1}$, with a = 7.6810 (6) Å, b = 9.9823 (6) Å, c = 10.7380 (9) Å, α = 96.83 (1)°, β = 93.28 (1)°, γ = 91.50 (1)°, and two formula units per unit cell. II is isostructural with I. III crystallized in the monoclinic system, space group $P2_1/n$, with a = 10.175 (7) Å, b = 21.478 (5) Å, c = 10.198 (8) Å, β = 97.41 (2)°, and four formula units per unit cell. Refinement by full-matrix least squares gave final residuals of R = 0.037 and R_w = 0.030 for I, R = 0.040 and R_w = 0.028 for II, and R = 0.043 and R_w = 0.033 for III. Cyclic voltammetry in DMF (glassy carbon electrode) shows single essentially nonreversible redox waves at positive potentials ($E_{1/2}$ = 0.41–0.47 V vs. SCE) associated with two-electron reduction.

Introduction

Binuclear, hydroxide-bridged copper(II) complexes of tetradentate (N_4) phthalazine and pyridazine ligands have copper–copper separations in the range 3.0–3.5 Å and Cu–O(H)–Cu bridge angles in the range 100–127°.[2-11] Variable-temperature magnetic studies have shown that strong antiferromagnetic cou-

* To whom correspondence should be addressed.
† This paper is assigned NRCC Contribution No. 26416.

(1) (a) Memorial University. (b) National Research Council. (c) Drexel University.
(2) Thompson, L. K.; Chacko, V. T.; Elvidge, J. A.; Lever, A. B. P.; Parish, R. V. *Can. J. Chem.* **1969**, *47*, 4141.
(3) Marongiu, G.; Lingafelter, E. C. *Acta Crystallogr. Sect. B: Struct. Crystallogr. Cryst. Chem.* **1982**, *B38*, 620.

0020-1669/87/1326-0657$01.50/0

pling exists between the copper(II) centers in complexes of this sort and that the exchange occurs via a superexchange mechanism with the hydroxide bridge acting as the primary pathway for exchange ($-2J$ = 200–800 cm^{-1}).[2,4-7] The magnitude of the exchange was found to vary in a linear manner with hydroxide bridge angle for a related series of complexes in which the N_4-$Cu_2(OH)$ binuclear fragment remains intact and the copper ions have $d_{x^2-y^2}$ ground states.[5,6] Two other unrelated, hydroxo-bridged, square-pyramidal copper(II) complexes involving macrocylic ligands[12,13] have been shown to approximate this relationship as well.[14] Structurally and magnetically complexes of this sort are considered to be effective models for the binuclear copper sites found in certain oxyhemocyanins. EXAFS studies on oxyhemocyanins suggest the presence of two or three histidines per metal center, with $d_{x^2-y^2}$ ground-state copper, and the likelihood of an oxygen group bridging the two metal centers, which are separated by 3.6 Å.[15-19] X-ray structural studies on Panulirus interruptus deoxyhemocyanin indicate that three histidine imidazoles are bound to each copper(I) center with the two copper atoms separated by 3.8 ± 0.4 Å.[20,21] Further, sequencing studies on various hemocynins suggest that tyrosine is not conserved in the domain in which the binuclear center is found, indicating that such a ligand (phenoxide) is unlikely to bridge the two copper centers in either the deoxy or oxy forms.[21]

The binuclear center dimensions in oxyhemocyanin (EXAFS) are consistent with an oxygen bridge angle of 145°,[18] and extrapolation of the linear relationship between hydroxide bridge angle and exchange integral for the hydroxo-bridged $d_{x^2-y^2}$ ground-state copper(II) complexes[14] gives $-2J$ = 1100 cm^{-1} (Cu–O–Cu = 145°) in close agreement with the observed value[22,23] and suggests that hydroxide acts as the magnetic protein bridge. Chemical and spectroscopic studies on tyrosinase indicate that its spin-coupled, type III, binuclear copper active site is similar to that found in the hemocyanins, and the spectroscopically effective model of the oxygenated active site contains two tetragonal copper(II) ions with nitrogen and oxygen (H_2O) donors and an oxygen bridge (phenolate, alkoxide, or hydroxide).[24-27] A similar active site structure is anticipated for the type III center found in laccase.[28]

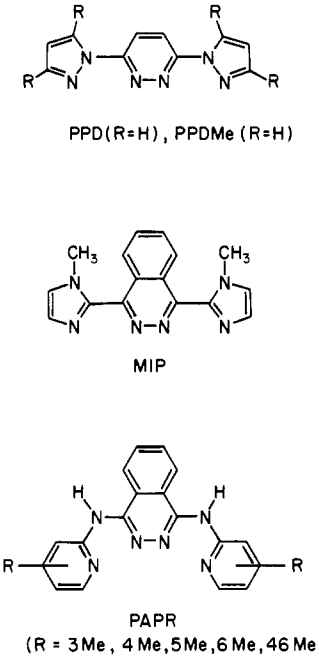

Figure 1. Structure of PPD, MIP, andd PAPR.

In order for "model" compounds to be considered as realistic mimics of protein active sites they must combine as many of the relevant physical properties as possible. Very few binuclear copper complexes, so far reported, combine relevant structural and magnetic properties with realistic electrochemical properties, a vitally important characteristic of the protein centers in terms of their ability to act as two-electron receptor sites. The type III copper protein centers, found in certain oxidases and oxygenases, typically exhibit positive reduction potentials and involve sequential two-electron transfer at the same potential (fungal laccase, $E_{1/2}$ = +782 mV;[29] tree laccase, $E_{1/2}$ = +434 mV;[29] tyrosinase, $E_{1/2}$ = 360 mV;[30] all potentials vs. SHE). Apart from the series of hydroxo-bridged, binuclear copper complexes of N_4-phthalazine and N_4-pyridazine ligands, reported by us, which exhibit positive reduction potentials in the range 0.3–0.8 V (vs. SCE) and involve two-electron reduction,[14,31,32] the antiferromagnetically coupled complex $[Cu_2(bpnp)(\mu\text{-}Cl)(\mu\text{-}OH)Cl_2]$ (bpnp = 2,7-bis(2-pyridyl)-1,8-naphthyridine) appears to be the only other system incorporating realistic structural and magnetic properties with positive reduction potentials ($E_{1/2}$ = 0.36, 0.16 V vs. Ag/AgCl in H_2O).[33] Positive redox potentials have, however, been observed for binuclear copper(II) complexes of "cryptate" ligands and other ligands with mixed NS donor sets,[34-37] which have essentially

(4) Thompson, L. K. *Can. J. Chem.* 1983, *61*, 579.
(5) Thompson, L. K.; Hartstock, F. W.; Robichaud, P.; Hanson, A. W. *Can. J. Chem.* **1984**, *62*, 2755.
(6) Thompson, L. K.; Hanson, A. W.; Ramaswamy, B. S. *Inorg. Chem.* **1984**, *23*, 2459.
(7) Thompson, L. K.; Woon, T. C.; Murphy, D. B.; Gabe, E. J.; Lee, F. L.; Le Page, Y. *Inorg. Chem.* **1985**, *24*, 4719.
(8) Ghedini, M.; De Munno, G.; Denti, G.; Manotti Lanfredi, A. M.; Tiripicchio, A. *Inorg. Chim. Acta* **1982**, *57*, 87.
(9) Dapporto, P.; De Munno, G.; Bruno, G.; Romeo, M. *Acta Crystallogr. Sect. C: Cryst. Struct. Commun.* **1983**, *C39*, 718.
(10) Dapporto, P.; De Munno, G.; Sega, A.; Mealli, L. *Inorg. Chim. Acta* **1984**, *83*, 171.
(11) De Munno, G.; Denti, G. *Acta Crystallogr. Sect C: Cryst. Struct. Commun.* **1984**, *C40*, 616.
(12) Burk, P. L.; Osborn, J. A.; Youinou, M.-T.; Agnus, Y.; Louis, R.; Weiss, R. *J. Am. Chem. Soc.* **1981**, *103*, 1273.
(13) Coughlin, P. K.; Lippard, S. J. *J. Am. Chem. Soc.* **1981**, *103*, 3228.
(14) Mandal, S. K.; Woon, T. C.; Thompson, L. K.; Newlands, M. J.; Gabe, E. J. *Aust. J. Chem.* **1986**, *39*, 1007.
(15) Co., M. S.; Hodgson, K. O.; Eccles, T. K.; Lontie, R. *J. Am. Chem. Soc.* **1981**, *103*, 984.
(16) Co, M. S.; Hodgson, K. O. *J. Am. Chem. Soc.* **1981**, *103*, 3200.
(17) Brown, J. M.; Powers, L.; Kincaid, B.; Larrabee, J. A.; Spiro, T. G. *J. Am. Chem. Soc.* **1980**, *102*, 4210.
(18) Woolery, G. L.; Powers, L.; Winkler, M.; Solomon, E. I.; Spiro, T. G. *J. Am. Chem. Soc.* **1984**, *106*, 86.
(19) Wilcox, D. E.; Long, J. R.; Solomon, E. I. *J. Am. Chem. Soc.* **1984**, *106*, 2186.
(20) Gaykema, W. P. J.; Hol, W. G. J.; Vereijken, J. M.; Soeter, N. M.; Bak, H. J.; Beintema, J. J. *Nature (London)* **1984**, *309*, 23.
(21) Hol, W. G. J.; Volbeda, A. *Rev. Port. Quim.* **1985**, *27*, 42.
(22) Solomon, E. I.; Dooley, D. M.; Wang, R.-H.; Gray, H. B.; Cerdonio, M.; Mogno, F.; Romani, G. L. *J. Am. Chem. Soc.* **1976**, *98*, 1029.
(23) Dooley, D. M.; Scott, R. A.; Ellinghaus, J.; Solomon, E. I.; Gray, H. B. *Proc. Natl. Acad. Sci. U.S.A.* **1978**, *75*, 3019.
(24) Eickman, N. C.; Solomon, E. I.; Larabee, J. A.; Spiro, T. G.; Lerch, K. *J. Am. Chem. Soc.* **1978**, *100*, 6529.
(25) Himmelwright, R. S.; Eickman, N. C.; LuBien, C. D.; Lerch, K.; Solomon, E. I. *J. Am. Chem. Soc.* **1980**, *102*, 7339.
(26) Jolley, R. L., Jr.; Evans, L. H.; Makino, N.; Mason, H. S. *J. Biol. Chem.* **1974**, *249*, 335.
(27) Jolley, R. L., Jr.; Evans, L. H.; Mason, H. S. *Biochem. Biophys. Res. Commun.* **1972**, *46*, 878.
(28) LuBien, C. D.; Winkler, M. E.; Thamann, T. J.; Scott, R. A.; Co, M. S.; Hodgson, K. O.; Solomon, E. I. *J. Am. Chem. Soc.* **1981**, *103*, 7014.
(29) Reinhammar, B. R. M. *Biochim. Biophys. Acta* **1972**, *275*, 245.
(30) Makino, N.; McMahill, P.; Mason, H. S. *J. Biol. Chem.* **1974**, *249*, 6062.
(31) Woon, T. C.; McDonald, R.; Mandal, S. K.; Thompson, L. K.; Addison, A. W. *J. Chem. Soc., Dalton Trans.* **1986**, 2381.
(32) Mandal, S. K.; Thompson, L. K.; Hanson, A. W. *J. Chem. Soc., Chem. Commun.* **1985**, 1709.
(33) Tikkanen, W. R.; Kruger, C.; Bomben, K. D.; Jolly, W. L.; Kaska, W. C.; Ford, P. C. *Inorg. Chem.* **1984**, *23*, 3633.
(34) Alberts, A. H.; Annunziata, R.; Lehn, J.-M. *J. Am. Chem. Soc.* **1977**, *99*, 8502.
(35) Gisselbrecht, J.-P.; Gross, M.; Albert, A. H.; Lehn, J.-M. *Inorg. Chem.* **1980**, *19*, 1386.
(36) Agnus, Y.; Louis, R.; Gisselbrecht, J.-P.; Weiss, R. *J. Am. Chem. Soc.* **1984**, *106*, 93.

Table I. Crystal Data

	$Cu_2C_{10}H_{11}Cl_3N_6O_2 \cdot 0.8H_2O$ (I)	$Cu_2C_{10}H_{11}Br_3N_6O_2 \cdot 0.6H_2O$ (II)	$Cu_2C_{16}H_{17}Br_3N_6O_2 \cdot H_2O$ (III)
cryst syst	triclinic	triclinic	monoclinic
space group	$P\bar{1}$	$P\bar{1}$	$P2_1/n$
a, Å	7.6810 (6)	7.7381 (20)	10.175 (7)
b, Å	9.9823 (6)	10.1462 (23)	21.478 (5)
c, Å	10.7380 (9)	11.151 (4)	10.198 (8)
α, deg	96.83 (1)	98.14 (2)	90.00
β, deg	93.28 (1)	93.93 (3)	97.41 (2)
γ, deg	91.50 (1)	90.93 (2)	90.00
V, Å^3	815.7	864.3	2210.04
Z	2	2	4
ρ(calcd), g cm^{-3}	2.018	2.401	2.120
μ, mm^{-1}	3.13	9.37	7.33
radiation; λ, Å	Mo Kα_1; 0.709 30	Mo Kα_1; 0.709 30	Mo Kα_1; 0.709 30
temp for data collcn, °C	22	22	22
min and max transmissn	0.45–0.75	0.40–0.81	0.58–0.64

magnetically isolated metal centers and no oxygen bridge groups, for the complexes $[Cu_2(bpy)_2(OH)_2]X_2$ (X = Cl, Br, BF_4; bpy = bipyridyl)[38] which contain a dihydroxy bridge, and for a trinuclear copper(II) derivative involving alkoxide bridges.[39] These sytems do not, however, structurally mimic protein centers.

In the present study we report the full structural details and electrochemical studies on the complexes $[Cu_2(PPD)(OH)X_3(H_2O)] \cdot nH_2O$ (X = Cl, n = 0.8; X = Br, n = 0.6) and $[Cu_2(MIP)(OH)Br_3(H_2O)] \cdot H_2O$ (PPD = 3,6-bis(1-pyrazolyl)-pyridazine; MIP = 1,4-bis(1-methyl-2-imidazolyl)phthalazine; Figure 1) and a variable-temperature (5–300 K) magnetic study on $[Cu_2(PPD)(OH)Cl_3(H_2O)] \cdot 0.8H_2O$. These binuclear, spin-coupled copper(II) complexes have square-pyramidal, hydroxide-bridged copper centers separated by 3.4–3.5 Å, with Cu–O(H)–Cu angles of 116–125°, and positive redox potentials (0.41–0.47 V vs. SCE), all features which make these systems relevant as binuclear copper protein analogues.

Experimental Section

Synthesis of Ligands and Copper Complexes. The syntheses of PPD[40] and MIP[5] and the complexes $[Cu_2(PPD)(OH)Cl_3(H_2O)] \cdot 0.8H_2O$ (I),[7] $[Cu_2(PPD)(OH)Br_3(H_2O)] \cdot 0.6H_2O$ (II),[7] and $[Cu_2(MIP)(OH)Br_3(H_2O)] \cdot H_2O$ (III)[5] have been reported previously. Satisfactory C, H, N analyses were obtained for all compounds studied.

Electrochemical Measurements. The electrochemical experiments were performed at room temperature in dimethylformamide (spectroscopic grade, dried over molecular sieves) under O_2-free conditions using a BAS CV27 voltammograph and a Houston omnigraph 2000 XY recorder. A three-electrode system was used (cyclic voltammetry) in which the working electrode was glassy carbon and the counter electrode platinum with a standard calomel (SCE) electrode as reference. For coulometry measurements a three-electrode system was employed consisting of a platinum mesh flag working electrode, a platinum mesh counter electrode, and a SCE reference electrode. The supporting electrolyte was tetraethylammonium perchlorate (TEAP) (0.1 M), and all solutions were 10^{-3}–10^{-4} in complex. The best combination of experimental conditions (working electrode, scan rates, solvent, etc.) was determined by preliminary experiment.

Magnetic Measurements. Room-temperature magnetic moments were measured by the Faraday method using a Cahn 7600 Faraday magnetic susceptibility system (compounds II, III). Varible-temperature magnetic susceptibility data were obtained in the range 5–300 K (compound I) by using an Oxford Instruments superconducting Faraday magnetic susceptibility system with a Sartorius 4432 microbalance. A main solenoid field of 1.5 T and a gradient field of 10 T m^{-1} were employed.

Crystallographic Data Collection and Refinement of the Structures. $[Cu_2(PPD)(OH)Cl_3(H_2O)] \cdot 0.8H_2O$ (I). Crystals of I are green. The diffraction intensities of an approximately 0.1 × 0.2 × 0.3 mm crystal were collected with graphite-monochromatized Mo Kα radiation by using the $\theta/2\theta$ scan technique with profile analysis[41] to $2\theta_{max}$ = 60° on a Picker four-circle diffractometer. A total of 5624 reflections were measured, of which 4764 were unique and 3549 reflections were considered significant with $I_{net} > 2.5\sigma(I_{net})$. Lorentz and polarization factors were applied, and absorption corrections were calculated. The cell parameters were obtained by the least-squares refinement of the setting angles of 48 reflections with $2\theta > 50°$ (λ(Mo Kα_1) = 0.709 30 Å).

Table II. Final Atomic Positional Parameters and Equivalent Isotropic Debye–Waller Temperature Factors (Esd's) for $[Cu_2(PPD)(OH)Cl_3(H_2O)] \cdot 0.8H_2O$ (I)

atom	x	y	z	B_{iso},[a] Å^2
Cu(1)	0.55662 (6)	0.71722 (4)	0.72847 (4)	2.836 (20)
Cu(2)	0.51198 (6)	0.37360 (4)	0.63867 (4)	2.669 (19)
Cl(1)	0.78916 (14)	0.84978 (11)	0.71984 (10)	4.33 (5)
Cl(2)	0.67451 (13)	0.25160 (10)	0.50567 (9)	3.71 (4)
Cl(3)	0.64500 (12)	0.31748 (9)	0.86718 (8)	3.06 (4)
O(1)	0.6535 (3)	0.54867 (18)	0.63673 (19)	4.36 (11)
N(1)	0.2573 (4)	0.8122 (3)	0.85196 (25)	2.51 (13)
N(2)	0.4127 (4)	0.8594 (3)	0.81529 (26	2.54 (12)
N(3)	0.3410 (3)	0.6104 (3)	0.76241 (24)	2.22 (12)
N(4)	0.3219 (3)	0.4791 (3)	0.72404 (24)	2.19 (12)
N(5)	0.3211 (4)	0.2336 (3)	0.63847 (26)	2.64 (13)
N(6)	0.1754 (4)	0.2782 (3)	0.69902 (25)	2.53 (12)
C(1)	0.1727 (6)	0.9119 (4)	0.9185 (4)	3.41 (18)
C(2)	0.2741 (6)	1.0247 (4)	0.9242 (4)	3.78 (19)
C(3)	0.4205 (6)	0.9894 (4)	0.8590 (4)	3.09 (17)
C(4)	0.2167 (4)	0.6757 (3)	0.8211 (3)	2.26 (14)
C(5)	0.0606 (5)	0.6114 (4)	0.8468 (3)	2.84 (17)
C(6)	0.0400 (5)	0.4768 (4)	0.8075 (3)	2.81 (17)
C(7)	0.1772 (4)	0.4141 (3)	0.7448 (3)	2.27 (14)
C(8)	0.0513 (5)	0.1775 (4)	0.6939 (4)	3.09 (17)
C(9)	0.1165 (6)	0.0668 (4)	0.6315 (4)	3.40 (18)
C(10)	2.813 (6)	0.1055 (4)	0.5985 (4)	3.30 (20)
O(2)	0.3294 (3)	0.36357 (25)	0.04214 (24)	3.92 (12)
O(3)	0.0399 (8)	0.39722 (54)	0.46575 (50)	11.53 (25)
H(1)	0.929 (5)	0.107 (4)	0.042 (3)	5.5 (11)
H(2)	0.741 (5)	−0.099 (4)	0.028 (3)	5.4 (11)
H(3)	0.485 (5)	−0.038 (4)	0.156 (3)	4.0 (10)
H(5)	1.027 (4)	0.338 (3)	0.116 (3)	3.1 (8)
H(6)	1.058 (4)	0.573 (3)	0.180 (3)	2.3 (8)
H(8)	1.055 (4)	0.805 (3)	0.268 (3)	3.6 (9)
H(9)	0.950 (4)	1.003 (3)	0.393 (3)	3.8 (9)
H(10)	0.652 (6)	0.933 (4)	0.437 (4)	4.9 (14)

[a] B_{iso} is the mean of the principal axes of the thermal ellipsoid.

The structure was solved by direct methods using MULTAN[42] and refined by full-matrix least-squares methods to final residuals of R = 0.037 and R_w = 0.030 for the significant data (0.058 and 0.030 for all data) with unit weights. Eight H atoms bound to carbon atoms of the ligand were located from difference maps. Crystal data are given in Table I, and final atomic positional parameters and equivalent isotropic temperature factors are listed in Table II. All calculations were performed with the NRCVAX system of programs.[43] Scattering factors were taken from ref 44. Anisotropic thermal parameters (Table SI) and

(37) Latour, J.-M.; Limosin, D.; Rey, P. *J. Chem. Soc., Chem. Commun.* **1985**, 464.
(38) Meyer, G.; Nadjo, L.; Lapinte, C. *Nouv. J. Chim.* **1984**, *8*, 777.
(39) Ferguson, G.; Langrick, C. R.; Parker, D.; Matthes, K. E. *J. Chem. Soc., Chem. Commun.* **1985**, 1609.
(40) Addison, A. W.; Burke, P. J. *J. Heterocycl. Chem.* **1981**, *18*, 803.
(41) Grant, D. F.; Gabe, E. J. *J. Appl. Crystallogr.* **1978**, *11*, 114.
(42) Germain, G.; Main, P.; Woolfson, M. M. *Acta Crystallogr., Sect. A: Cryst. Phys. Diffr., Theor. Gen. Crystallogr.* **1971**, *A27*, 368.
(43) Gabe, E. J.; Lee, F. L.; Le Page, Y. *Crystallographic Computing III*; Sheldrick, G., Kruger, C., Goddard, R., Eds.; Clarendon Press: Oxford, 1985; p 167.
(44) *International Tables for X-ray Crystallography*; Kynoch Press: Birmingham, England, 1974; Vol IV, Table 2.2B, p 99.

Table III. Final Atomic Positional Parameters and Equivalent Isotropic Debye–Waller Temperature Factors (Esd's) for $[Cu_2(PPD)(OH)Br_3(H_2O)]\cdot 0.6H_2O$ (II)

atom	x	y	z	B_{iso},[a] Å^2
Cu(1)	0.44512 (16)	0.28510 (12)	0.26894 (11)	3.15 (6)
Cu(2)	0.48231 (16)	0.62109 (12)	0.35703 (11)	3.02 (6)
Br(1)	0.20413 (15)	0.15029 (12)	0.28798 (11)	4.84 (6)
Br(2)	0.30743 (14)	0.74163 (11)	0.49731 (9)	3.71 (5)
Br(3)	0.34614 (14)	0.68691 (11)	0.12907 (9)	3.30 (5)
O(1)	0.3512 (7)	0.4511 (5)	0.3532 (5)	5.1 (3)
N(1)	0.7410 (10)	0.1883 (7)	0.1495 (7)	2.4 (4)
N(2)	0.5882 (10)	0.1436 (8)	0.1832 (7)	3.0 (4)
N(3)	0.6548 (10)	0.3890 (7	0.2360 (7)	2.5 (4)
N(4)	0.6708 (10)	0.5186 (7)	0.2738 (6)	2.4 (4)
N(5)	0.6710 (10)	0.7588 (8)	0.3620 (7)	2.9 (4)
N(6)	0.8120 (11)	0.7177 (8)	0.3047 (7)	2.7 (4)
C(1)	0.8247 (12)	0.0883 (10)	0.0836 (9)	3.2 (5)
C(2)	0.7252 (14)	−0.0207 (10)	0.0771 (9)	3.6 (6)
C(3)	0.5854 (13)	0.0169 (10)	0.1396 (8)	3.1 (5)
C(4)	0.7780 (12)	0.3260 (9)	0.1800 (7)	2.4 (5)
C(5)	0.9339 (12)	0.3887 (9)	0.1573 (8)	2.9 (5)
C(6)	0.9507 (13)	0.5231 (10)	0.1965 (9)	3.3 (5)
C(7)	0.8145 (12)	0.5851 (10)	0.2582 (8)	2.3 (5)
C(8)	0.9306 (12)	0.8174 (10)	0.3095 (8)	3.4 (5)
C(9)	0.8640 (14)	0.9273 (10)	0.3710 (9)	3.5 (5)
C(10)	0.6992 (14)	0.8850 (10)	0.4012 (9)	3.5 (5)
O(2)	0.6805 (9)	0.6429 (6)	0.9596 (6)	4.4 (4)
O(3)	0.0502 (26)	0.4305 (18)	0.4785 (18)	13.4 (9)
H(1)	0.955 (0)	0.099 (0)	0.042 (0)	4.1 (0)
H(2)	0.752 (0)	−0.119 (0)	0.029 (0)	4.4 (0)
H(3)	0.477 (0)	−0.056 (0)	0.152 (0)	3.9 (0)
H(5)	1.037 (0)	0.332 (0)	0.109 (0)	3.5 (0)
H(6)	1.072 (0)	0.577 (0)	0.181 (0)	4.2 (0)
H(8)	1.059 (0)	0.811 (0)	0.269 (0)	4.1 (0)
H(9)	0.929 (0)	1.029 (0)	0.393 (0)	4.1 (0)
H(10)	0.609 (0)	0.954 (0)	0.453 (0)	3.9 (0)

[a] B_{iso} is the mean of the principal axes of the thermal ellipsoid.

a listing of structure factors (Table SII) are included as supplementary material.

$[Cu_2(PPD)(OH)Br_3(H_2O)]\cdot 0.6H_2O$ (II). Crystals of II are dark green. The diffraction intensities of an approximately 0.2 × 0.1 × 0.18 mm crystal were collected with graphite-monochromatized Mo Kα radiation by using the $\theta/2\theta$ scan technique with profile analysis[41] to $2\theta_{max} = 50°$ on a Picker four-circle diffractometer. Of 3052 unique reflections 1923 were considered significant with $I_{net} > 2.5\sigma(I_{net})$. Lorentz and polarization factors were applied, and absorption corrections were calculated. The cell parameters were obtained by the least-squares refinement of the setting angles of 54 reflections with $2\theta > 40°$ (λ(Mo Kα_1) = 0.709 30 Å). The structure was solved as for I to final residuals of $R = 0.040$ and $R_w = 0.028$ for the significant data (0.090 and 0.029 for all data). The positions of the H atoms bound to carbon atoms of the ligand were calculated. Crystal data are given in Table I, and final atomic positional parameters and equivalent isotropic temperature factors are listed in Table III. Anisotropic thermal parameters (Table SIII) and a listing of structure factors (Table SIV) are included as supplementary material.

$[Cu_2(MIP)(OH)Br_3(H_2O)]\cdot H_2O$ (III). Crystals of III are dark green. The diffraction intensities of an approximately 0.12 × 0.10 × 0.10 mm crystal were collected with graphite-monochromatized Mo Kα radiation by using the Ω scan technique to $2\theta_{max} = 49°$ on a Nonius CAD4 diffractometer. Of a total of 4424 measured reflections 3873 were unique and 1656 were considered significant with $I_{net} > 2.5\sigma(I_{net})$. Lorentz and polarization factors were applied, and absorption corrections were calculated. The cell parameters were obtained by the least-squares refinement of the setting angles of 25 reflections with $2\theta > 30°$ (λ(Mo Kα_1) = 0.709 30 Å). The structure was solved as for I to final residuals of $R = 0.043$ and $R_w = 0.033$ for the significant data (0.157 and 0.037 for all data). The positions of the H atoms bound to carbon atoms of the ligand were calculated. Crystal data are given in Table I, and final atomic positional parameters and equivalent isotropic temperature factors are listed in Table IV. Anisotropic thermal parameters (Table SV) and a listing of structure factors (Table SVI) are included as supplementary material.

Results and Discussion

Tetradentate, N_4, binucleating ligands involving disubstituted heterocyclic diazine fragments in general form binuclear copper complexes, and in many cases the two copper centers are bridged

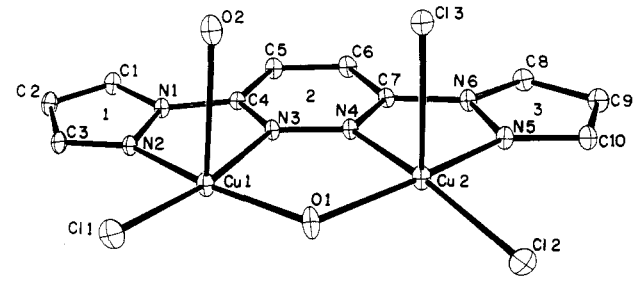

Figure 2. Structural representation of $[Cu_2(PPD)(OH)Cl_3(H_2O)]\cdot 0.8H_2O$ (I) with hydrogen atoms omitted (40% probability thermal ellipsoids).

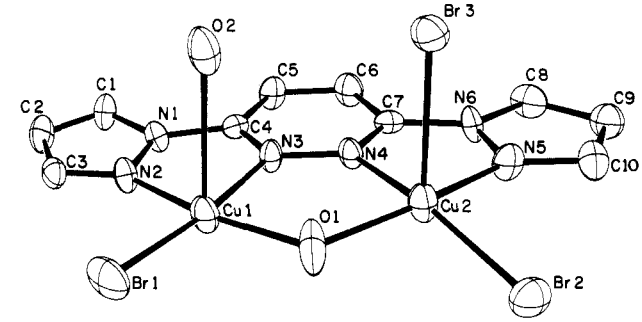

Figure 3. Structural representation of $[Cu_2(PPD)(OH)Br_3(H_2O)]\cdot 0.6H_2O$ (II) with hydrogen atoms omitted (40% probability thermal ellipsoids).

by hydroxide in addition to the diazine moiety. Various diazine groups have been used including phthalazine,[2-7,14,32] pyridazine,[7-11,31,32] and triazole.[45] In the case of the ligand 3,5-bis(pyridin-2-yl)-1,2,4-triazole (bptH) a series of binuclear (1:1) complexes are formed, $Cu_2(bpt)_2X_2(H_2O)_{2-4}$ (X = CF_3SO_3, ClO_4, NO_3, BF_4), in which the two metal centers are bound simultaneously between two adjacent tetradentate ligands, with axial perturbations by both water molecules and the anion (X = CF_3SO_3).[45] This structural arrangement is unique among the ligands in question, and in all other cases reported 2:1 (metal:ligand) complexes are produced. The tetradentate phthalazine complexes (ligands PAPR; Figure 1) form (2:1) binuclear copper complexes that are almost exclusively hydroxide-bridged,[2-7,14,32] while for binuclear copper complexes of the pyrazolyl pyridazines PPD and PPDME (Figure 1) hydroxide-bridged species have resulted, so far, in all cases. This contrasts somewhat with the situation for the analogous pyridazine ligand 3,6-bis(pyridin-2-yl)pyridazine (DPPN) that produced hydroxide-bridged binuclear copper(II) complexes[8-11] but also, in one case, a chloro-bridged derivative.[46,47]

Description of the Structures of $[Cu_2(PPD)(OH)Cl_3(H_2O)]\cdot 0.8H_2O$ (I), $[Cu_2(PPD)(OH)Br_3(H_2O)]\cdot 0.6H_2O$ (II), and $[Cu_2(MIP)(OH)Br_3(H_2O)]\cdot H_2O$ (III). The structure of I is shown in Figure 2, and interatomic distances and angles relevant to the copper coordination spheres are given in Table V. The binuclear, neutral complex is essentially flat with two copper(II) atoms bound to four in-plane (N_2OCl) donors with Cu–N and Cu–O distances close to 2.0 Å and Cu–Cl distances in excess of 2.2 Å. Weak axial perturbations (Cu(1)–O(2) (H_2O) = 2.783 Å, Cu(2)–Cl(3) = 2.729 Å) indicate that the stereochemistry at each copper center is square-pyramidal, but significant distortion exists in the square plane itself. Cu(1) lies 0.041 Å below the mean plane defined by the basal atoms while Cu(2) lies 0.201 Å above the equivalent mean plane. A significant equatorial compression of each plane results from the very acute angles N(2)–Cu(1)–N(3) (77.8°) and

(45) Prins, R.; Birker, P. J. M. W. L.; Haasnoot, J. G.; Verschoor, G. C.; Reedijk, J. *Inorg. Chem.* **1985**, *24*, 4128.
(46) De Munno, G.; Denti, G.; Dapporto, P. *Inorg. Chim. Acta* **1983**, *74*, 199.
(47) De Munno, G.; Bruno, G. *Acta Crystallogr., Sect. C: Cryst. Struct. Commun.* **1984**, *C40*, 2022.

Table IV. Final Atomic Positional Parameters and Equivalent Isotropic Debye–Waller Temperature Factors (Esd's) for $[Cu_2(MIP)(OH)Br_3(H_2O)]\cdot H_2O$ (III)

atom	x	y	z	B_{iso},[a] Å^2
Cu(1)	0.31736 (15)	0.52104 (8)	0.87014 (16)	2.20 (8)
Cu(2)	0.26440 (16)	0.36397 (7)	0.87914 (16)	2.36 (9)
Br(1)	0.39469 (15)	0.57326 (7)	0.68928 (15)	3.64 (8)
Br(2)	0.23244 (14)	0.29713 (7)	0.69164 (14)	3.18 (8)
Br(3)	−0.00320 (13)	0.39388 (7)	0.90526 (16)	3.31 (8)
O(1)	0.3050 (7)	0.4391 (3)	0.7904 (8)	2.3 (4)
O(2)	0.4060 (8)	0.0344 (4)	0.6717 (9)	4.1 (5)
H(202)	0.9925 (11)	0.2980 (6)	0.1807 (13)	9.9 (8)
N(1)	0.3421 (9)	0.5918 (5)	0.9995 (11)	1.9 (6)
N(2)	0.3917 (9)	0.6218 (5)	1.2067 (11)	2.0 (6)
N(3)	0.3202 (10)	0.4755 (5)	1.0443 (12)	2.4 (6)
N(4)	0.3093 (9)	0.4144 (5)	1.0510 (10)	1.9 (5)
N(5)	0.3515 (10)	0.2708 (6)	1.2219 (12)	2.4 (6)
N(6)	0.2781 (10)	0.2970 (5)	1.0158 (11)	2.6 (6)
C(1)	0.3819 (13)	0.6524 (6)	0.9990 (15)	2.6 (7)
C(2)	0.4105 (13)	0.6728 (6)	1.1272 (16)	2.7 (7)
C(3)	0.3467 (12)	0.5732 (7)	1.1257 (16)	2.4 (8)
C(4)	0.4400 (13)	0.6209 (7)	1.3505 (13)	2.7 (7)
C(5)	0.3114 (12)	0.5094 (6)	1.1534 (14)	1.9 (7)
C(6)	0.2630 (12)	0.4849 (6)	1.2681 (13)	1.8 (6)
C(7)	0.2128 (12)	0.5191 (6)	1.3642 (14)	2.3 (7)
C(8)	0.1595 (12)	0.4894 (7)	1.4646 (13)	2.7 (8)
C(9)	0.1490 (13)	0.4251 (7)	1.4691 (14)	2.4 (7)
C(10)	0.1953 (12)	0.3911 (7)	1.3731 (13)	2.4 (7)
C(11)	0.2526 (11)	0.4176 (7)	1.2711 (14)	2.2 (7)
C(12)	0.2900 (11)	0.3848 (6)	1.1604 (14)	1.8 (6)
C(13)	0.3037 (12)	0.3180 (6)	1.1408 (13)	1.8 (6)
C(14)	0.3518 (14)	0.2188 (7)	1.1497 (17)	3.5 (8)
C(15)	0.3105 (13)	0.2362 (7)	1.0189 (15)	2.7 (8)
C(16)	0.4103 (18)	0.2767 (6)	1.3621 (18)	3.4 (9)
H(1)	0.393 (0)	0.682 (0)	0.910 (0)	3.3 (0)
H(2)	0.438 (0)	0.720 (0)	1.163 (0)	3.4 (0)
H(4A)	0.523 (10)	0.645 (5)	1.370 (11)	3.6 (0)
H(4B)	0.459 (0)	0.573 (0)	1.382 (0)	3.4 (0)
H(4C)	0.361 (0)	0.638 (0)	1.405 (0)	3.4 (0)
H(7)	0.214 (0)	0.571 (0)	1.360 (0)	3.0 (0)
H(8)	0.125 (0)	0.518 (0)	1.546 (0)	3.4 (0)
H(9)	0.103 (0)	0.403 (0)	1.549 (0)	3.2 (0)
H(10)	0.187 (0)	0.339 (0)	1.377 (0)	3.1 (0)
H(14)	0.380 (0)	0.170 (0)	1.185 (0)	4.1 (0)
H(15)	0.306 (0)	0.204 (0)	0.931 (0)	3.4 (0)
H(16A)	0.406 (15)	0.249 (6)	1.402 (15)	3.6 (0)
H(16B)	0.388 (0)	0.322 (0)	1.398 (0)	3.6 (0)
H(16C)	0.520 (0)	0.275 (0)	1.364 (0)	3.6 (0)

[a] B_{iso} is the mean of the principal axes of the thermal ellipsoid.

Table V. Interatomic Distances (Å) and Angles (deg) Relevant to the Copper Coordination Spheres in $[Cu_2(PPD)(OH)Cl_3(H_2O)]\cdot 0.8H_2O$ (I)[a]

Bond Distances			
Cu(1)–O(1)	2.028 (1)	Cu(2)–O(1)	2.034 (1)
Cu(1)–N(3)	2.020 (3)	Cu(2)–N(4)	2.021 (3)
Cu(1)–N(2)	1.997 (3)	Cu(2)–N(5)	1.998 (3)
Cu(1)–Cl(1)	2.208 (1)	Cu(2)–Cl(2)	2.225 (1)
Cu(1)–O(2)	2.783 (1)	Cu(2)–Cl(3)	2.729 (1)
Cu(1)–Cu(2)	3.454 (1)		

Bond Angles			
O(1)–Cu(1)–N(3)	90.2 (1)	O(1)–Cu(2)–N(4)	89.7 (1)
N(3)–Cu(1)–N(2)	77.8 (1)	N(4)–Cu(2)–N(5)	77.4 (1)
N(2)–Cu(1)–Cl(1)	95.8 (1)	N(5)–Cu(2)–Cl(2)	96.2 (1)
Cl(1)–Cu(1)–O(1)	96.6 (1)	Cl(2)–Cu(2)–O(1)	94.8 (1)
O(1)–Cu(1)–N(2)	167.5 (1)	O(1)–Cu(2)–N(5)	165.1 (3)
N(3)–Cu(1)–Cl(1)	171.5 (1)	N(4)–Cu(2)–Cl(2)	166.3 (1)
O(1)–Cu(1)–O(2)	90.2 (1)	O(1)–Cu(2)–Cl(3)	96.3 (1)
N(3)–Cu(1)O(2)	81.2 (1)	N(4)–Cu(2)–Cl(3)	89.8 (1)
N(2)–Cu(1)–O(2)	90.9 (1)	N(5)–Cu(2)–Cl(3)	91.0 (1)
Cl(1)–Cu(1)–O(2)	93.4 (1)	Cl(2)–Cu(2)–Cl(3)	102.6 (1)
Cu(1)–O(1)–Cu(2)	116.4 (1)		

[a] Esd's are given in parentheses.

N(4)–Cu(2)–N(5) (77.4°). The pyrazole and pyridazine rings (1, 2, 3; Figure 2) are almost coplanar (1–2, 3.4°; 1–3, 4.5°; 2–3, 3.6°) with an angle of 6.0° between the mean planes of the basal donor sets. The copper–copper separation is 3.454 Å with an angle of 116.4° at the bridging oxygen. The hydrogen atom bound to O(1) could not be located, but other data leave little doubt as to the identity of this bridge as hydroxide.[7]

Table VI. Interatomic Distances (Å) and Angles (deg) Relevant to the Copper Coordination Spheres in $[Cu_2(PPD)(OH)Br_3(H_2O)]\cdot 0.6H_2O$ (II)[a]

Bond Distances			
Cu(1)–O(1)	1.983 (1)	Cu(2)–O(1)	1.981 (1)
Cu(1)–N(3)	2.003 (7)	Cu(2)–N(4)	2.008 (7)
Cu(1)–N(2)	2.002 (8)	Cu(2)–N(5)	1.997 (8)
Cu(1)–Br(1)	2.334 (2)	Cu(2)–Br(2)	2.361 (2)
Cu(1)–O(2)	2.861 (2)	Cu(2)–Br(3)	2.856 (2)
Cu(1)–Cu(2)	3.413 (2)		

Bond Angles			
O(1)–Cu(1)–N(3)	89.4 (2)	O(1)–Cu(2)–N(4)	88.8 (2)
N(3)–Cu(1)–N(2)	77.7 (3)	N(4)–Cu(2)–N(5)	77.1 (3)
N(2)–Cu(1)–Br(1)	97.4 (2)	N(5)–Cu(2)–Br(2)	97.9 (2)
Br(1)–Cu(1)–O(1)	95.6 (1)	Br(2)–Cu(2)–O(1)	94.0 (1)
O(1)–Cu(1)–N(2)	167.0 (2)	O(1)–Cu(2)–N(5)	163.9 (2)
N(3)–Cu(1)–Br(1)	174.0 (2)	N(4)–Cu(2)–Br(2)	166.0 (2)
O(1)–Cu(1)–O(2)	89.8 (1)	O(1)–Cu(2)–Br(3)	98.0 (1)
N(3)–Cu(1)–O(2)	81.9 (2)	N(4)–Cu(2)–Br(3)	90.0 (2)
N(2)–Cu(1)–O(2)	90.1 (2)	N(5)–Cu(2)–Br(3)	89.8 (2)
Br(1)–Cu(1)–O(2)	94.8 (1)	Br(2)–Cu(2)–Br(3)	103.1 (1)
Cu(1)–O(1)–Cu(2)	118.9 (1)		

[a] Esd's are given in parentheses.

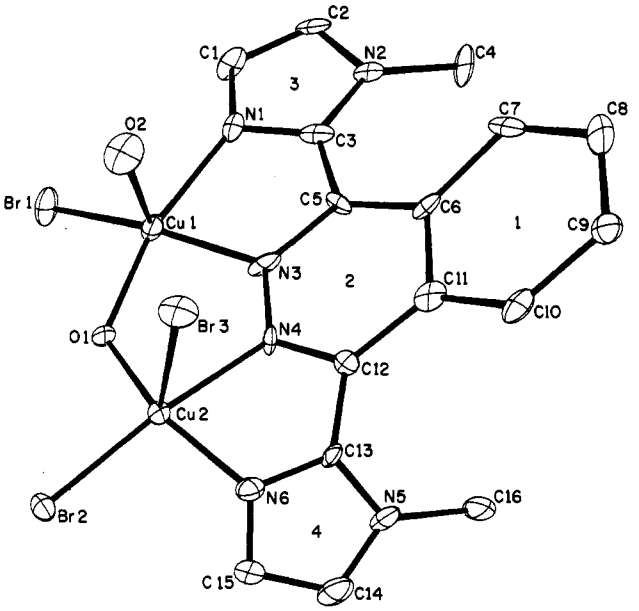

Figure 4. Structural representation of $[Cu_2(MIP)(OH)Br_3(H_2O)]\cdot H_2O$ (III) with hydrogen atoms omitted (30% probability thermal ellipsoids).

The structure of II is shown in Figure 3, and interatomic distances and angles relevant to the copper coordination spheres are given in Table VI. I and II are isostructural with very similar overall geometry and dimensions involving the ligand and the two metal centers. The copper–halogen bond lengths are significantly longer in II with an axial Cu(2)–Br(3) separation of 2.856 Å. The copper–axial water distance of 2.861 Å is also significantly longer than that in I. The copper–copper separation (3.413 Å) is slightly shorter than that in I, but shorter bond lengths to the oxygen bridge result in a significantly larger Cu(1–O(1)–Cu(2) bridge angle (118.9°).

The structure of III is shown in Figure 4, and interatomic distances and angles relevant to the copper coordination spheres are given in Table VII. The stereochemistry at each copper center is approximately square-pyramidal with the same arrangement of donor atoms in the basal plane (N_2OBr) with a relatively short Cu(1)–O(2) separation but a very long axial copper–bromine

Table VII. Interatomic Distances (Å) and Angles (deg) Relevant to the Copper Coordination Spheres in $[Cu_2(MIP)(OH)Br_3(H_2O)]\cdot H_2O$ (III)[a]

	Bond Distances		
Cu(1)–O(1)	1.936 (7)	Cu(2)–O(1)	1.921 (8)
Cu(1)–N(3)	2.025 (11)	Cu(2)–N(4)	2.061 (10)
Cu(1)–N(1)	2.007 (10)	Cu(2)–N(6)	1.995 (11)
Cu(1)–Br(1)	2.378 (3)	Cu(2)–Br(2)	2.380 (2)
Cu(1)–O(2)	2.276 (2)	Cu(2)–Br(3)	2.843 (3)
Cu(1)–Cu(2)	3.420 (2)		
	Bond Angles		
O(1)–Cu(1)–N(3)	85.5 (4)	O(1)–Cu(2)–N(4)	85.5 (4)
N(3)–Cu(1)–N(1)	78.6 (5)	N(4)–Cu(2)–N(6)	78.3 (5)
N(1)–Cu(1)–Br(1)	97.3 (3)	N(6)–Cu(2)–Br(2)	96.7 (3)
Br(1)–Cu(1)–O(1)	96.5 (3)	Br(2)–Cu(2)–O(1)	98.3 (3)
O(1)–Cu(1)–N(1)	163.8 (4)	O(1)–Cu(2)–N(6)	159.2 (4)
Br(1)–Cu(1)–N(3)	160.0 (3)	Br(2)–Cu(2)–N(4)	173.1 (3)
O(1)–Cu(1)–O(2)	91.5 (2)	O(1)–Cu(2)–Br(3)	97.0 (2)
N(3)–Cu(1)–O(2)	97.3 (3)	N(4)–Cu(2)–Br(3)	84.9 (3)
N(1)–Cu(1)–O(2)	93.8 (3)	N(6)–Cu(2)–Br(3)	94.5 (3)
Br(1)–Cu(1)–O(2)	102.6 (1)	Br(2)–Cu(2)–Br(3)	100.3 (1)
Cu(1)–O(1)–Cu(2)	124.9 (4)		

[a] Esd's are given in parentheses.

separation (Cu(2)–Br(3) = 2.843 Å). The basal planes are rather distorted with an equatorial compression at the acute angles N(1)–Cu(1)–N(3) (78.6°) and N(4)–Cu(2)–N(6) (78.3°). Also the copper centers are raised above the mean planes of the basal donor sets (Cu(1), 0.245 Å; Cu(2), 0.160 Å). The copper–copper separation is 3.420 Å and the Cu(1)–O(1)–Cu(2) angle 124.9°. The ligand itself is severely twisted with an angle of 12.4° between the phthalazine best planes 1 and 2, angles of 25.2 and 34.3°, respectively, between imidazole rings 3 and 4 and the phthalazine plane 2, and an angle of 30.8° between the imidazole planes themselves. The twisting of the ligand is, no doubt, due to steric interactions between the imidazole *N*-methyl groups and protons H(7) and H(10) on the phthalazine moiety.

Structurally complexes I and II can be compared with binuclear copper complexes of DPPN and in particular $[Cu_2(DPPN)(OH)Cl_3(H_2O)]$[8] and $[Cu_2(DPPN)(OH)Br_3]_n$,[10] which have similar structures in which the two square-pyramidal copper(II) centers are bridged by a hydroxide and involve terminal copper–halogen bonds and axial interactions with chlorine and water and bromines. However, despite the overall general similarity in the structures, especially the Cu–NN(diazine)–Cu framework, there is a striking difference in the dimensions of the Cu–O–Cu bridging framework. Compounds I and II have angles N(3)–Cu(1)–O(1) and N(4)–Cu(2)–O(1) close to 90° with Cu–O(1) separations close to 2.0 Å, whereas for the DPPN complexes significantly shorter Cu–O separations and smaller N–Cu–O angles result in Cu–O–Cu bridge angles (126.5°, Cl; 128.1°, Br) that are 10° larger. A comparable bridge angle (Cu–O–Cu = 126.0°) has been reported for $[Cu_2(PPDMe)(OH)Cl_2][CuCl_3(H_2O)]\cdot H_2O$[7] involving the ligand 3,6-bis(3,5-dimethyl-1-pyrazolyl)pyridazine. The presence of a methyl group adjacent to the peripheral nitrogen donor site in N_4 ligands of this sort has been shown to have a dramatic effect on Cu–O–Cu bridge angles in complexes of the ligands PAP and PAP6Me (Figure 1). The complex $[Cu_2(PAP)(OH)Cl_3]\cdot 1.5H_2O$[3] has a Cu–O–Cu bridge angle of 100.0° whereas a bridge angle of 112.2° is observed for $[Cu_2(PAP6Me)(OH)Cl_3]\cdot 3H_2O$.[32] Compound III has a very similar structure to $[Cu_2(MIP)(OH)Cl_3(H_2O)]\cdot H_2O$ in which the interplanar ligand angles and the stereochemistries at the copper centers are comparable but the hydroxide bridge angle is slightly larger (126.3°).[5] This large bridge angle leads to the presence of strong antiferromagnetic exchange for the chloro derivative ($-2J$ = 800 cm^{-1})[5] with a room-temperature magnetic moment (μ_{eff}) of 0.50 μ_β.

Magnetism. Room-temperature magnetic moments for I (μ_{eff} = 0.42 μ_β, this work), II, and III (DIAM)[7] indicate very strong antiferromagnetic coupling between the copper(II) centers. Magnetic susceptibility measurements were performed on a powdered sample of $[Cu_2(PPD)(OH)Cl_3(H_2O)]\cdot 0.8H_2O$ (I) in the temperature range 5–300 K. The results are summarized in Figure 5. The best-fit line was calculated from the Van Vleck equation[48] for exchange-coupled pairs of copper(II) ions (eq 1).

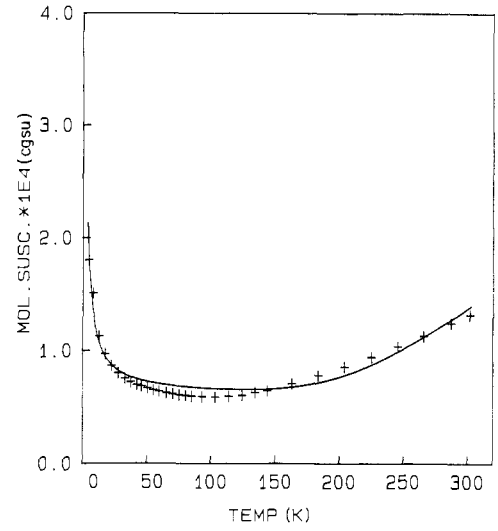

Figure 5. Magnetic susceptibility data for $[Cu_2(PPD)(OH)Cl_3(H_2O)]\cdot 0.8H_2O$ (I). The solid line was calculated from eq 1 with g = 2.16 ± 0.04, $-2J$ = 898 ± 13 cm^{-1}, and $N\alpha$ = 60 × 10^{-6} cgs units (cm^3 mol^{-1})/Cu and assuming 0.14% paramagnetic impurity (ρ = 0.0014).

$$\chi_M = \frac{N\beta^2g^2}{3kT}\left[1 + \frac{1}{3}\{\exp(-2J)\}\right]^{-1}(1-\rho) + \left[\frac{N\beta^2g^2}{4kT}\right]\rho + N\alpha \quad (1)$$

In this expression $2J$ (in th *spin* Hamiltonian $H = 2J\hat{s}_1\hat{s}_2$) is the singlet–triplet splitting or exchange integral, and other symbols have their usual meaning. ρ represents the fraction of a possible magnetically dilute copper(II) impurity. The temperature-independent paramagnetism for a binuclear copper(II) complex, $N\alpha$, was taken as 120 × 10^{-6} cgs units/mol. The parameters giving the best fit were obtained by using a nonlinear regression analysis with ρ as a floating parameter. The exchange integral for I (900 cm^{-1}) indicates very strong antiferromagnetic exchange between the copper(II) centers. The apparent diamagnetism of compounds II and III suggests that in these systems spin exchange is even stronger.

The pyridazine-bridged complexes I and II therefore do not fit the linear relationship between hydroxide bridge angle and exchange integral that has been demonstrated for related hydroxo-bridged phthalazine complexes with $d_{x^2-y^2}$ copper ion ground states.[5,6,14] The exchange appears to be somewhat larger for the pyridazine complexes on the basis of a comparison of hydroxide bridge angles. However, further magnetic studies on other derivatives, especially at variable temperatures, will be necessary to fully substantiate this. In a recent report it has been demonstrated that reasonable estimates of exchange integrals can be obtained from room temperature effective magnetic moments for binuclear copper(II) complexes by suitable substitution into the Van Vleck exchange equation.[49] Using the parameters g = 2.16, T = 301.8 K, μ_{eff} = 0.42 μ_B, and 0.14% paramagnetic impurity gave $-2J$ = 915 cm^{-1}, in close agreement with the value obtained from the variable-temperature magnetic study for I.

The binuclear copper complexes I and II have two square-pyramidal copper(II) centers bridged by a nitrogen fragment (pyridazine) and a single oxygen atom (hydroxide) involving a five-membered, essentially flat, Cu_2N_2O ring. A similar ring is found in III that is slightly puckered. The projected structure for the oxyhemocyanin active site involves a similar five-membered dicopper ring with comparable dimensions, but with dioxygen in

(48) Van Vleck, J. H. *The Theory of Electric and Magnetic Suceptibilities*; Oxford University Press: London, 1932; Chapter 9.
(49) Thompson, L. K.; Ramaswamy, B. S. *Inorg. Chem.* **1986**, *25*, 2664.

Table VIII. Electrochemical Data

compd	scan rate, mV s^{-1}	ΔE_p, mV	$E_{1/2}$, V vs. SCE
$[Cu_2(PPD)(OH)Cl_3(H_2O)]\cdot 0.8H_2O$ (I)	50[a]	125	0.41
	100	135	
	200	140	
	300	155	
	400	175	
	500	190	
$[Cu_2(PPD)(OH)Br_3(H_2O)]\cdot 0.6H_2O$ (II)	200[a]	140	0.47
$[Cu_2(MIP)(OH)Br_3(H_2O)]\cdot H_2O$ (III)	100[a]	140	0.44
	200	160	
	300	175	

[a] 3×10^{-3} to 3×10^{-4} M complex in DMF, 0.1 M tetraethylammonium perchlorate, glassy carbon working electrode, and saturated calomel reference electrode.

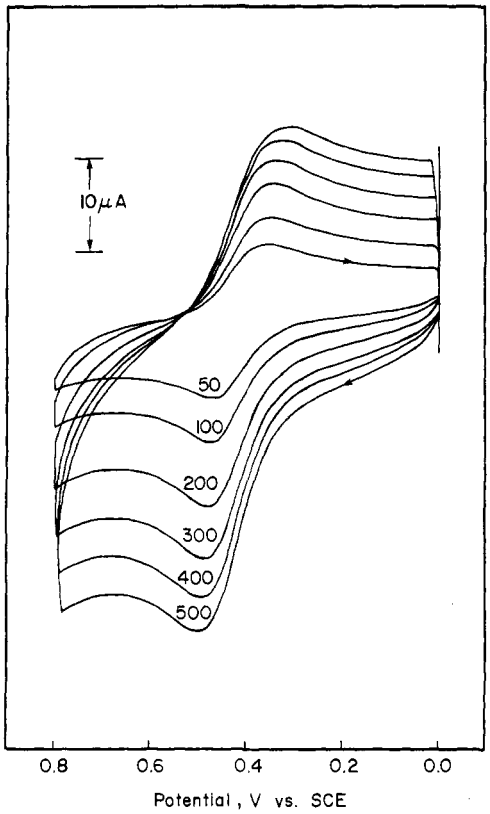

Figure 6. Cyclic voltammograms for $[Cu_2(PPD)(OH)Cl_3(H_2O)]\cdot 0.8H_2O$ (I) in DMF (3×10^{-3} M, 0.1 M TEAP, GC, SCE, 50–500 mV s^{-1}).

place of the diazine dinitrogen fragment and two square-pyramidal copper(II) centers bound to histidine imidazole ligands. The single atom oxygen bridging ligand, thought to be largely responsible for the diamagnetism of oxyhemocyanin, is considered realistically to be either phenoxide (tyrosine) or more likely hydroxide.[50] Despite the fact that in I, II, and III the donors are not the same as those expected in the oxyhemocyanins, from a geometrical standpoint these complexes are realistic protein structural mimics. This is borne out also by the magnetic properties of these systems that emphasize the role of the hydroxide bridge as the principal exchange pathway in such species.

Electrochemistry. Electrochemical data for I–III are reported in Table VIII. Cyclic voltammetry in dried DMF gave single redox waves for each compound with $E_{1/2}$ values in the range 0.41–0.47 V (vs. SCE). Figure 6 shows cyclic voltammograms at varying scan rates for $[Cu_2(PPD)(OH)Cl_3(H_2O)]\cdot 0.8H_2O$ in DMF. ΔE_p values vary significantly as a function of scan rate,

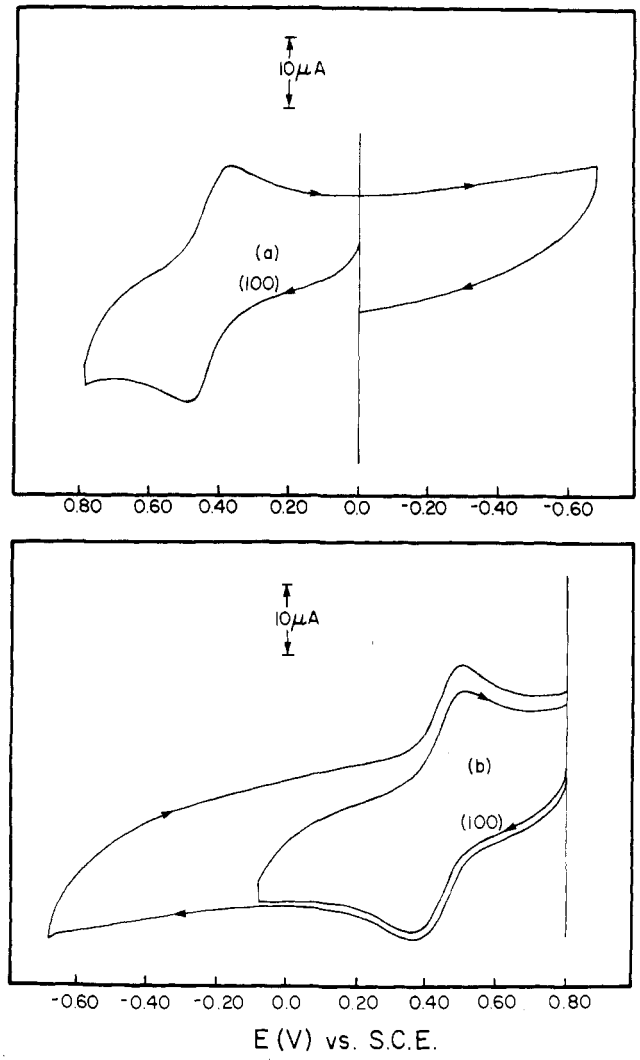

Figure 7. Cyclic voltammograms for $[Cu_2(PPD)(OH)Cl_3(H_2O)]\cdot 0.8H_2O$ (I) in DMF (3×10^{-3} M, 0.1 M TEAP, GC, SCE; 100 mV s^{-1}): (a) positive scan from 0.0 V; (b) negative scan from +0.8 V.

indicating an essentially nonreversible redox process. Similarly compounds II and III exhibited essentially nonreversible redox processes. Identical cyclic voltammograms were obtained by sweeping the potential in a positive direction from 0.0 to +0.8 V and from +0.8 to 0.0 V for I (parts a and b, respectively, of Figure 7) and in the range 0.0 to +0.65 V for II (Figure 8b,c). A similar situation was observed for III. No electrochemical activity is apparent for I, II, or III in the range 0.0 → −0.7 V (Figure 7 and 8). Additional, irreversible oxidations observed above +0.80 (I) and +0.65 V (II and III) are associated with oxidation of chloride and bromide, respectively. Controlled potential electrolysis of green solutions of II and III (platinum electrode at +0.10 V vs. SCE) in DMF gave electron counts that correspond to less than 2 equiv of charge (approximately 1.5) with the formation of almost colorless solutions that exhibited no visible absorption associated with copper(II) species. Compound I was found to have limited solubility in DMF and was not studied coulometrically. However it is assumed to involve a redox process identical with that of II. The reduced coulomb counts are attributed to a spontaneous redox reaction involving the solvent in which some of the complex is reduced to copper(I). Such a situation is supported by a time-dependent study of the visible absorption of these complexes in DMF. A significant, but relatively slow, decrease is observed in the intensity of the visible bands, with no appearance of bands attributable to other copper(II) species. Reoxidation of fully reduced solutions of II and III at +0.60 V restored the green color, with d–d absorption spectra identical with those observed initially and required approximately 2 equiv of charge. Further reduction of the reoxidized solution of II at +0.1 V produced an almost

(50) Reed, C. A. In *Biological and Inorganic Copper Chemistry*; Karlin, K. D., Zubieta, J., Eds.; Adenine Press: New York, 1986; Vol. 1, p 61.

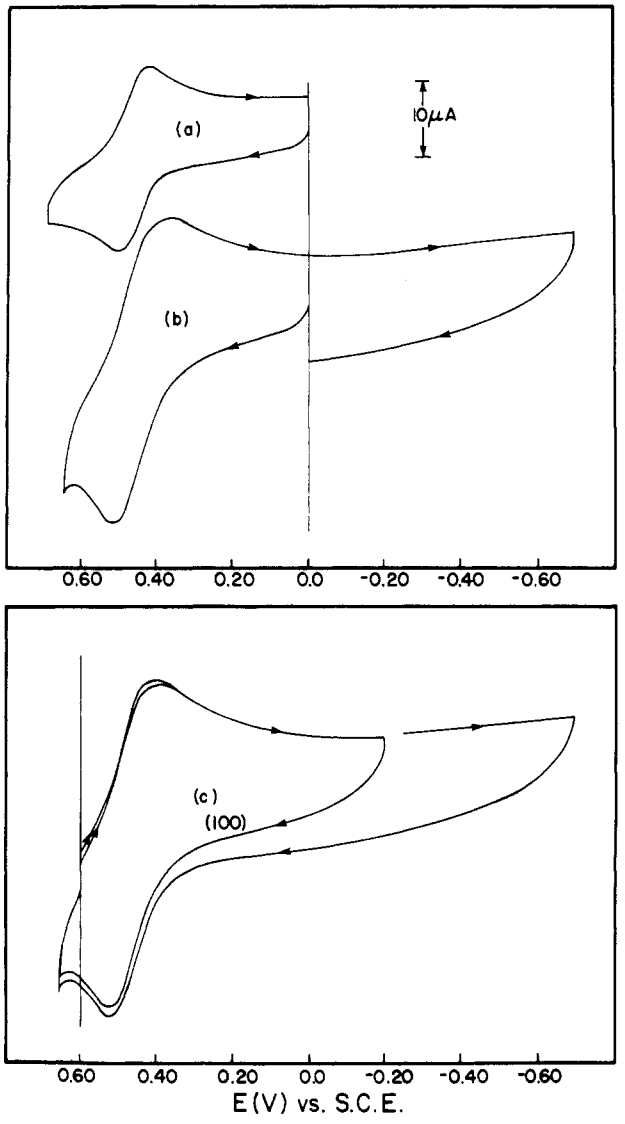

Figure 8. Cyclic voltammograms for $[Cu_2(PPD)(OH)Br_3(H_2O)]\cdot 0.6H_2O$ (II) in DMF (3×10^{-3} M, 0.1 M TEAP, GC, SCE; 100 mV s^{-1}): (a) ferrocene/ferrocinium couple; (b) positive scan from 0.0 V; (c) negative scan from 0.6 (0.65) V.

colorless solution with passage of 2 equiv of charge. Cyclic voltammograms for this solution, sweeping the potential in both positive and negative directions within the limits 0.0 and +0.6 V, were found to be identical with those observed for the initial binuclear copper(II) species.

Reduced coulomb counts on coulometric reduction of binuclear copper(II) phthalazine complexes with positive reduction potentials have been observed in acetonitrile ($E_{1/2}$ values approximately, +0.8 V)[14] and undried DMF ($E_{1/2}$ values 0.4–0.5 V)[14] and are attributed to partial reduction of the complex by the solvent. We have not, as yet, been able to isolate or detect any oxidized solvent species. Such a sitution is rare, but is not unprecedented in the case of acetonitrile,[51,52] and is likely to be a result of the high redox potentials observed for these complexes.

Electrochemical studies have shown that in general negative reduction potentials (vs. SCE) prevail for binuclear copper(II) complexes involving oxygen atom bridges,[53-58] even though in many cases strong antiferromagnetic exchange is observed. Positive reduction potentials, comparable with those of the type III copper protein centers, have been observed for antiferromagnetically coupled, hydroxide-bridged, binuclear copper(II) complexes of tetradentate (N_4) diazine ligands[14,31,32] and a related naphthyridine (N_4) ligand,[33] and in all cases the copper centers are part of six-membered chelate rings. Reversible and quasi-reversible redox processes are observed for many of these systems, which are attributed in part to the flexibility imparted to the systems by the ligands that form these six-membered chelate rings (see Figure 1; PAPR). Compounds I, II, and III are therefore further examples of what is a small group of such systems, but with five-membered chelate rings. The lack of electrochemical reversibility associated with the redox processes for I, II, and III can be attributed in part to their rigid, planar structures, which would not accommodate the likely geometrical changes that would accompany reduction as easily. It is therefore suggested that the binuclear copper protein centers, which exhibit reversible redox processes, are likely to involve stereochemically flexible donor sets that are not constrained by the formation of small chelate rings.

Acknowledgment. We thank the Natural Sciences and Engineering Research Council of Canada for financial support for this study including the purchase of the variable-temperature Faraday susceptometer.

Supplementary Material Available: Listings of anisotropic thermal parameters for I, II, and III (Tables SI, SIII, and SV) and bond length and angle data pertaining to the ligands in I, II, and III (Tables SVII, SVIII, and SIX) (8 pages); listings of observed and calculated structure factors for I, II, and III (Tables SII, SIV, SVI) (81 pages). Ordering information is given on any current masthead page.

(51) Nelson, S. M.; Esho, F.; Lavery, A.; Drew, M. G. B. *J. Am. Chem. Soc.* **1983**, *105*, 5693.
(52) Drew, M. G. B.; Yates, P. C.; Trocha-Grimshaw, J.; McKillop, K. P.; Nelson, S. M. *J. Chem. Soc., Chem. Commun.* **1985**, *262*.
(53) Lintvedt, R. L.; Stecher Kramer, L. *Inorg. Chem.* **1983**, *22*, 796.
(54) Fenton, D. E.; Schroeder, R. R.; Lintvedt, R. L. *J. Am. Chem. Soc.* **1978**, *100*, 1931.
(55) Mandal, S. K.; Nag, K. *Inorg. Chem.* **1983**, *22*, 2567.
(56) Mandal, S. K.; Nag, K. *J. Chem. Soc., Dalton Trans* **1983**, 2429.
(57) Cabral, J. DeO.; Cabral, M. F.; McCann, M.; Nelson, S. M. *Inorg. Chim. Acta* **1984**, *86*, L15.
(58) Mazurek, W.; Bond, A. M.; Murray, K. S.; O'Connor, M. J.; Wedd, A. G. *Inorg. Chem.* **1985**, *24*, 2484.